Journal of Magnetism and Magnetic Materials 189 (1998) 101–105

Femtosecond spin dynamics probed by linear and nonlinear magneto-optics

W. Hübner, G.P. Zhang*

Max-Planck-Institut für Mikrostrukturphysisik, Weinberg 2, D-06120 Halle, Germany

Received 17 March 1998; received in revised form 22 May 1998

Abstract

A theoretical study is performed on ultrafast spin dynamics as probed by linear and nonlinear (magneto-)optics, such as second harmonic generation (SHG). Both intrinsic spin and charge dynamics occur on a time scale of 10 fs. A clear delay of spin dynamics with respect to charge dynamics is observed. Such delay is clear not only for the linear response, but also for the nonlinear response such as $\chi^{(2)}$. We find that the different pump pulse shape could result in a different dynamical process. And for a larger probe frequency, the oscillatory behavior of the spin dynamics is clearer, the period is shorter, and the decay time is longer. All of these effects show that one can actively tune the dynamics by properly choosing the experimental conditions. Our study provides some insights into ultrafast spin dynamics. © 1998 Elsevier Science B.V. All rights reserved.

PACS: 75.40.Gb; 75.70.−i; 78.20.Ls; 78.47.+p

Keywords: Femtosecond spin dynamics; Ferromagnetic system; Linear and nonlinear magneto-optical responses

1. Introduction

Fundamental importance and potential applications of fast magneto-optical recording greatly motivate experimental as well as theoretical studies. Although an early experiment yielded a spin relaxation time of Gd as long as 100 ps [1], where basically the spin-lattice interaction plays an important role, and the so-called spin density wave can be considered as a quasi-particle with a well-defined temperature, this stimulated one to investigate the spin dynamics on a faster time scale. Beaurepaire et al. [2] were the first to observe the spin dynamics on the time scale less than (1 ps in nickel. A sharp decrease of magnetization is recently observed on the time scale less than 100 fs in $CoPt_3$ [3] and nickel [4]. By contrast, theoretical calculations are very few [5]. This is partly due to the fact that these ferromagnetic metals belong to a typical strongly correlated system [6], thus one has to employ a rather sophisticated scheme to treat correlation effects. This is especially true when

* Corresponding author. Tel.: + 49 345 5582 649; fax: + 49 345 5511 223; e-mail: zhang@mpi-halle.mpg.de.

PII: S0304-8853(98)00218-2

one studies the spin dynamics on an ultrafast time scale.

In this article, we employ a theoretical scheme to examine the spin dynamics. Our theoretical results show that (1) the ultrafast spin dynamics occurs on the time scale of 10 fs; (2) the spin dynamics lags behind the charge dynamics; (3) the spin dynamics depends on the external parameters such as pump pulse shapes and probe frequencies.

2. Theory

We start with a generic Hamiltonian which includes the band structure, electron exchange interaction and spin–orbit coupling. The Hamiltonian reads as follows:

$$H = \sum_{i,j,k,l,\sigma,\sigma',\sigma'',\sigma'''} U_{i\sigma,j\sigma',l\sigma''',k\sigma''} c^{\dagger}_{i\sigma} c^{\dagger}_{j\sigma'} c_{k\sigma''} c_{l\sigma'''} + \sum_{\nu,\sigma,\kappa} \mathscr{E}_{\nu}(K) n_{\nu\sigma}(K) + H_{\mathrm{SO}} \quad (1)$$

where $U_{i\sigma,j\sigma',l\sigma''',k\sigma''}$ is the electron interaction, which can be described in full generality by the three parameters Coulomb repulsion U, exchange interaction J, and the exchange anisotropy ΔJ [7,8]. $c^{\dagger}_{i\sigma}(c_{i\sigma})$ are the usual creation (annihilation) operators in the orbital i with spin σ ($\sigma = \uparrow, \downarrow$). $\mathscr{E}_{\nu}(K)$ is the single-particle energy spectrum for band ν. $n_{\nu\sigma}(K)$ is the particle number operator in momentum space. H_{SO} is the spin–orbit coupling [9]. A Hamiltonian of this kind is general enough to address the spin dynamics on the ultrafast time scale. However it is not possible to solve it without further approximations. Fortunately, in the magneto-optical process, vertical (momentum conserving) transitions dominate the whole spectra. Thus, we ignore those terms of the electron interaction, which are off-diagonal in momentum space. Under the above approximation, we are able to solve the Hamiltonian by the exact diagonaloza-tion scheme.

To have a clear view of the intrinsic origin of the dynamics, firstly we calculate $S_z(t) = \langle \Psi(0)|\hat{S}_z|\Psi(t)\rangle$ and $N(t) = \langle \Psi(0)|\hat{N}|\Psi(t)\rangle$, which represent the spin and charge dynamics, respectively. $|\Psi(0)\rangle$ is the initial state; $|\Psi(t)\rangle = \mathrm{e}^{-\mathrm{i}Ht/\hbar}|\Psi(0)\rangle$; $\hat{S}_z$ is the spin operator in the z direction; $\hat{N}$ is the electron number operator.

To calculate the experimental observables probed at a fixed delay time, we use $\chi^{(1)}_{xy}$, $\chi^{(1)}_{zz}$, $\chi^{(1)}_{xzz}$ and $\chi^{(2)}_{zzz}$. Their expressions are defined as follows:

$$\chi^{(1)}_{xy}(\omega, t) = \sum_{k,l,l'} \frac{p(E_{kl}, t) - p(E_{kl'}, t)}{\omega - (E_{kl} - E_{kl'}) + \mathrm{i}\eta} \times (\langle kl|\hat{S}_z|kl\rangle + \langle kl'|\hat{S}_z|kl'\rangle - 1), \quad (2)$$

$$\chi^{(1)}_{zz}(\omega, t) = \sum_{k,l,l'} \frac{p(E_{kl}, t) - p(E_{kl'}, t)}{\omega - (E_{kl} - E_{kl'}) + \mathrm{i}\eta}, \quad (3)$$

$$\chi^{(2)}_{xzz}(\omega, t) = \sum_{k,l,l',l''} \left(\frac{p(E_{kl''}, t) - p(E_{kl'}, t)}{E_{kl''} - E_{kl'} - \omega + \mathrm{i}\eta} - \frac{p(E_{kl'}, t) - p(E_{kl}, t)}{E_{kl'} - E_{kl} - \omega + \mathrm{i}\eta} \right) /(E_{kl''} - E_{kl} - 2\omega + \mathrm{i}2\eta)(\langle kl|\hat{S}_z|kl\rangle + \langle kl'|\hat{S}_z|kl'\rangle + \langle kl''|\hat{S}_z|kl''\rangle - 3/2), \quad (4)$$

$$\chi^{(2)}_{zzz}(\omega, t) = \sum_{k,l,l',l''} \left(\frac{p(E_{kl''}, t) - p(E_{kl'}, t)}{E_{kl''} - E_{kl'} - \omega + \mathrm{i}\eta} - \frac{p(E_{kl'}, t) - p(E_{kl}, t)}{E_{kl'} - E_{kl} - \omega + \mathrm{i}\eta} \right) /(E_{kl''} - E_{kl} - 2\omega + \mathrm{i}2\eta), \quad (5)$$

where $|kl\rangle$ is the eigenstate with the eigenvalue E_{kl}; $p(E_{kl}, t) = \langle \Psi(t)|kl\rangle$. $\chi^{(1)}_{xy}$ (magneto-optical Kerr effect) and $\chi^{(2)}_{xzz}$ (nonlinear magneto-optical Kerr effect) reflect the response of spin dynamics while $\chi^{(1)}_{zz}$ (reflectivity) and $\chi^{(2)}_{zzz}$ (SHG signal) reflect the response of charge dynamics.

3. Results

Before we come to the experimental observables, we firstly calculate some intrinsic quantities, namely $S_z(t)$ and $N(t)$ to see how the spin and charge dynamics occur on the very short time scale. In Fig. 1, we show a typical evolution of $|S_z(t)|$ and $|N(t)|$ with time. Both $|S_z(t)|$ and $|N(t)|$ decrease sharply within 100 fs. Such a decay results from the dephasing of the initial state. We note that even if $\hat{S}_z$ and $\hat{N}$ are good quantum numbers, one still can

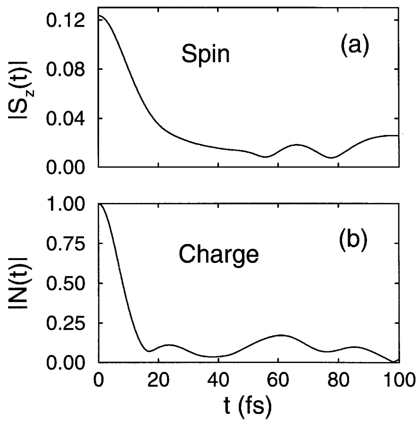

Fig. 1. Intrinsic physical quantities, (a) $|S_z(t)|$ and (b) $|N(t)|$, as a function of time t. The initial state is prepared 2 eV above the ground state with a Gaussian broadening 0.1 eV.

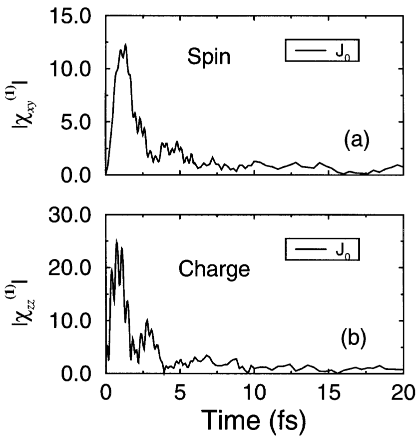

Fig. 2. (a) Linear magneto-optical and (b) optical responses change with time. The pump frequency is 2 eV with the excited state prepared with a broadening 20 eV.

see the decay since the loss of coherence between different eigenstates leads to a decay of observables. A careful survey shows a difference between spin and charge dynamics, namely the spin dynamics lags behind the charge dynamics. For this specific set of parameters (the pump frequency is 2 eV, the initial excited state Gaussian broadening 0.1 eV), the spin dynamics decays on the time scale of 50 fs while for the charge dynamics a sharp decay occurs less than 20 fs. Thus the spin dynamics delays about 30 fs. Such a delay is very important as it gives spin memory time, a time during which magnetic information can be written on the disk. As we will see below, such a delay is also clear either between $|\chi^{(1)}_{zz}|$ and $|\chi^{(1)}_{xy}|$ or between $|\chi^{(2)}_{zzz}|$ and $|\chi^{(2)}_{xzz}|$.

In Fig. 2, we plot the susceptibilities $|\chi^{(1)}_{xy}(\omega, t)|$ and $|\chi^{(1)}_{zz}(\omega, t)|$ with time. The probe frequency ω is taken to be 2 eV. The initial state distribution width is chosen as broad as 20 eV in order to investigate the intrinsic speed limit of spin dynamics. Here again we observe a very fast decay for both $|\chi^{(1)}_{zz}|$ and $|\chi^{(1)}_{xy}|$ on the time scale of 4 fs. If one compares $|\chi^{(1)}_{zz}|$ with $|\chi^{(1)}_{xy}|$ carefully, a delay of $|\chi^{(1)}_{xy}|$ with respect to $|\chi^{(1)}_{zz}|$ can be noted. For this set of specific parameters, we estimate that the relaxation time for the charge dynamics is about 4 fs while for the spin dynamics about 6 fs. To understand the origin of the delay qualitatively, we invoke a single-particle picture [10]. When light hits the material, electrons are excited out of the Fermi sea. Whenever electrons go back to the Fermi sea, one sees the charge dynamics. However one can observe the dynamics only if the electron scatters into the Fermi sea with its spin orientation changed. This process needs higher orders of interactions between electrons. Thus, the probability becomes very small. It takes time for electrons to find a right position to fill in, which consequently delays the spin dynamics.

With the same set of parameters as above, we also calculate $|\chi^{(2)}_{xzz}(\omega, t)|$ and $|\chi^{(2)}_{zzz}(\omega, t)|$. In Fig. 3, we plot the results up to 20 fs. Once again one observes a rapid decrease for both spin ($|\chi^{(2)}_{xzz}(\omega, t)|$) and charge ($|\chi^{(2)}_{zzz}(\omega, t)|$) dynamics on the time scale of 10 fs; the charge dynamics also finishes faster than the spin dynamics. It is important to realize that on such short time scale, the lattice is not involved in the dynamics. The spin dynamics occurs due to the dephasing of the initial excited state.

Up to now, all the excited state distributions are Gaussians. Next we study how different kinds of initial state distributions affect the spin dynamics. In Fig. 4, we make a comparison between the Gaussian distribution and Fermi distribution. Here $\omega = 2$ eV. In the insets of the figure, the initial state populations are plotted as a function of energy. For convenience, we replot the results with the initial state prepared by a Gaussian function in Fig. 4a. In Fig. 4b, the initial state distribution is prepared

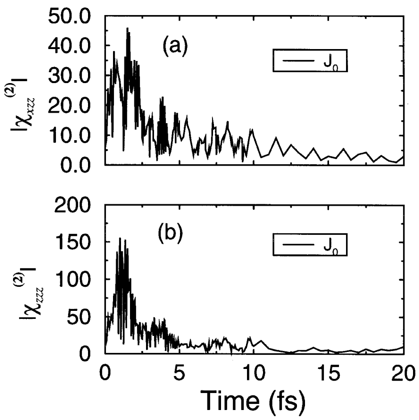

Fig. 3. (a) Nonlinear magneto-optical and (b) optical responses change with time. The same parameters are used as those in Fig. 2.

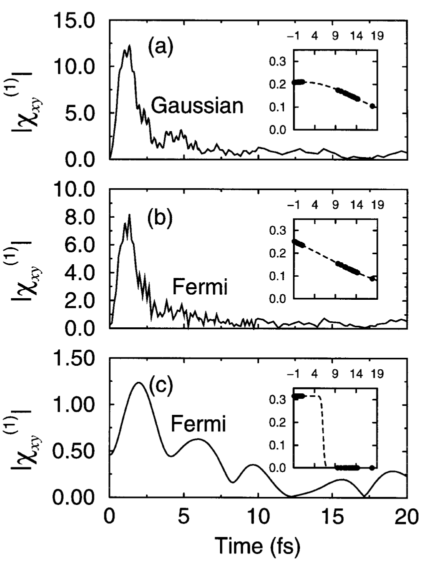

Fig. 4. Different laser pulse shapes affect the spin dynamics: (a) the initial excited state is populated according to a Gaussian function; (b) and (c) the initial states are populated according to a Fermi distribution with $\beta = 0.1$/eV and 5/eV, respectively. Insets: abscissa and coordinate refer to the energy spectra (in units of eV) and populations for different distributions.

according to a Fermi distribution, $f(E) = 1/(e^{\beta(E-E_0)} + 1)$, where $\beta = 0.1$/eV and E_0 is used to shift the center of the distribution. For this particular distribution, all the states are populated, but the relative weight is different. From the figure, one can observe that $|\chi_{xy}^{(1)}|$ decreases within 10 fs. The results are very similar to those in Fig. 4a, but a slightly longer decay is observed. Next, we choose $\beta =$ 5/eV. Fig. 4c displays the results. There are several differences. Firstly, the spin dynamics decays slower. The decay time exceeds 10 fs. At the early stages, we can observe three clear oscillations, which indicate that the coherence is still present. This is very different from the case with $\beta = 0.1$/eV where one cannot see such a clear recurrence. This difference is understandable. From the inset of Fig. 4c, one may notice that this distribution is close to a 'low-temperature' Fermi distribution, namely only the states within the 'Fermi ball' are populated. The number of populated states is smaller than that in Fig. 4b. The loss of coherence is not as strong as that in the case of Fig. 4b. Consequently one can see the recurrence. This concludes that the pulse shape and laser fluence also affect the observed dynamics.

Moreover for a typical pump–probe experiment [2], it is expected that the probe frequency should also impact on our observation. Here we provide a detailed comparison. The shape of the initial state distribution is also a Fermi distribution. We choose the probe frequencies, $\omega_{pb} = 0.1$, 1.0, 2.0 and 8.0 eV. $\beta = 5$/eV. We plot the results up to 20 fs. The first observation from Fig. 5a–Fig. 5d is that as the probe frequency increases, the first drop is shifted from 5.5 fs for $\omega_{pb} = 0.1$ eV (Fig. 5d) to 3.4 fs for $\omega_{pb} = 8$ eV (Fig. 5a). This means that, as expected, the oscillation occurs with a shorter period as the probe frequency increases. For the second drop, the same thing happens: the drop occurs at 7.4 fs for $\omega_{pb} = 8$ eV (Fig. 5a), and delays to 9.4 fs for $\omega_{pb} =$ 0.1 eV (Fig. 5d). Moreover this drop becomes sharper as the probe frequency increases. The oscillatory behavior is clearer for a larger probe frequency since the number of accessible levels is reduced. For $\omega_{pb} = 8$ eV, three cycles, are observed before it relaxes to the final position; for $\omega_{pb} = 0.1$ eV, after roughly two cycles, $|\chi_{xy}^{(1)}|$ reaches its ultimate value. We find that the decay time is shorter for smaller probe frequencies. For $\omega_{pb} = 0.1$ eV, we estimate that the decay time is about 10 fs while for $\omega_{pb} = 8$ eV, it is longer than 20 fs. Therefore, we conclude that in experiments, the observed

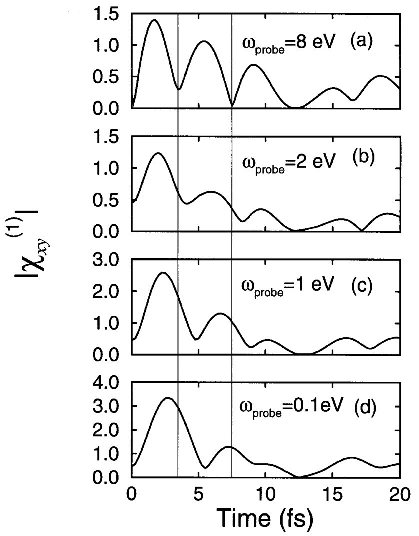

Fig. 5. Different probe frequencies affect the final observation. The initial state is prepared according to a Fermi distribution with $\beta = 5$/eV.

relaxation process can be affected by choosing different probe frequencies.

In conclusion, we provide a theoretical study of spin dynamics on an ultrafast time scale. This time scale is well beyond the characteristic time of spin-lattice interaction. We observe that both intrinsic spin and charge dynamics occur on a time scale of 10 fs, but a clear delay of spin dynamics with respect to charge dynamics is observed. This delay is important as it gives the spin memory time. A number of external parameters influence the spin dynamics. For the pump pulse, different shapes lead to different initial excited state distributions. We find that the spin dynamics with a Gaussian populated initial state is different from that with a Fermi distribution populated initial state. For a larger β, the spin dynamics slows down. Concerning the probe pulse frequency, we notice that for a larger probe frequency, the oscillatory behavior is clearer, the period is shorter, and the decay time is longer. All these effects are vital to the experiments since they will influence final observations. Our study shows that one can actively tune the dynamics by properly choosing the experimental conditions.

References

[1] A. Vaterlaus, T. Beutler, F. Meier, Phys. Rev. Lett. 67 (1991) 3314.

[2] E. Beaurepaire, J.-C. Merle, A. Daunois, J.Y. Bigot, Phys. Rev. Lett. 76 (1996) 4250.

[3] E. Beaurepaire, J.-C. Merle, A. Daunois, J.Y. Bigot, unpublished.

[4] J. Hohlfeld, E. Matthias, R. Knorren, K.H. Bennemann, Phys. Rev. Lett. 78 (1997) 4861.

[5] W. Hübner, K.H. Bennemann, Phys. Rev. B 53 (1996) 3422.

[6] P. Fulde, Electron Correlation in Molecules and Solids, 3rd ed., Springer, Heidelberg, 1995.

[7] W. Hübner, L.M. Falicov, Phys. Rev. B 47 (1993) 8783.

[8] C. Moore, Atomic Energy Levels, Natl. Bur. Stand. (US) (US GPO, Washington, DC, 1971).

[9] H. Takayama, K. Bohnen, P. Fulde, Phys. Rev. B 14 (1976) 2287.

[10] G.D. Mahan, Many-Particle Physics, 2nd ed., Plenum Press, New York, 1990.